

Optimal cell-to-cell active balancing using fuzzy type-2 BEC implemented zeta and quasi-resonant buck converters on Li-ion based battery pack

Indhana Sudiharto, Farid Dwi Murdianto, Vena Chika Widyasavitta

Department of Electrical Engineering, Politeknik Elektronika Negeri Surabaya, Surabaya, Indonesia

Article Info

Article history:

Received Jan 7, 2024

Revised Jun 3, 2024

Accepted Jun 20, 2024

Keywords:

Active balancing

Cell-to-cell balancing

Fuzzy type-2

Quasi-resonant buck converter

Zeta converter

ABSTRACT

Many motorized vehicles use non-environmentally friendly fuels causing more pollution. To tackle this, electric vehicles with battery technology are becoming popular. Many electric cars use Li-ion battery packs. However, these battery packs can have differences between individual batteries, affecting their performance. When electric cars accelerate, the batteries can get imbalanced, which shortens their lifespan. To prevent this, a balancing circuit is needed to make sure each battery cell stays equal. To get the balancing current according to the needs of each battery cell and switching network components. As a result, this research creates a cell-to-cell active balancing using the quasi-resonant buck converter that can reduce ripple from zeta converter output. Fuzzy type-2-BEC adjusts the duty cycle zeta converter circuits. The output is set equal to the average cell voltage. Four pieces of Li-ion are connected in the series at 14.4 V/3 Ah. To test the balancers, two variations were used to determine the system's reliability. From the test result, variation one can balance all cells at the 60 s, and variation two can balance all cells at the 150 s.

This is an open access article under the [CC BY-SA](#) license.



Corresponding Author:

Indhana Sudiharto

Department of Electrical Engineering, Politeknik Elektronika Negeri Surabaya

Raya ITS St.- PENS Campus Sukolilo, Surabaya, 60111, Indonesia

Email: indhana@pens.ac.id

1. INTRODUCTION

The growth of motorized vehicles and fuel oil fossil consumption continuously increases yearly [1]. The use of fuels that are not environmentally friendly encourages the emergence of electric vehicle innovations using battery technology [2]. Many electric vehicles extensively utilize Lithium-Ion batteries [3], [4]. Li-ion batteries have several advantages compared to lead acid batteries, such as lighter weight, faster charging time, higher density, and higher security. Charging and discharging cycles in Li-ion batteries cause different cell voltages [5], [6]. In a vehicle, both acceleration and deceleration take place. When acceleration is applied, the regenerative braking system in electric cars is engaged. This system is designed to discharge the battery during acceleration, leading to an imbalance in the battery pack [7], [8]. This situation is specifically relevant when an electric vehicle is accelerating, as only one of the batteries is drained and not evenly distributed. So, a balancing circuit is needed to equalize each cell battery [9]. Balancing batteries is categorized into two methods: passive balancing and active balancing [10], [11]. Passive balancing functions by linking resistors in parallel to individual battery cells, dissipating energy as heat through these resistors [12]. This balancing approach features a straightforward circuit design that is easy to produce, employs cost-effective components, and has a compact circuit size [13].

On the other hand, this method wastes energy which causes a burden on the thermal management of battery cells. Active balancing evens out the voltage among each battery cell by moving charges from cells with higher voltage to those with lower voltage [14]. This balancing method is more efficient than passive balancing but has a more complicated circuit than passive balancing, and the cost of making the circuit is high [15]. This problem can be solved by using the cell-to-cell battery balancing with a quasi-resonant buck converter that can reduce ripple from zeta converter output. A zeta converter can adjust the source voltage to a higher or lower value to obtain a balancing current according to the needs of each battery cell and switching network component. Four pieces of Li-ion battery are used which are connected in series. With this method, it is hoped that it can overcome the problem of imbalance between battery cells in a battery pack during the charging and discharging process, which can cause a decrease in battery performance.

2. RESEARCH METHOD

In this stage, the zeta converter and quasi-resonant buck converter balance the battery pack. The design and manufacture of systems consisting of Li-ion batteries, zeta converter, quasi-resonant buck converter, and fuzzy type-2-BEC designs can be seen in Figure 1. Figure 1 explains the diagram block of the cell balancing system. An active balancing circuit system is used to distribute energy from cells that have maximum energy to cells that have minimum energi [16]. This research uses a Li-ion battery as its power source, so a control method is needed to keep the battery in a balanced state during the discharge process [17]. Using Li-ion batteries as a source can use one battery cell. The balancing process is carried out to maintain the lifetime of the Li-ion battery to avoid over-discharge which affects battery life[18].

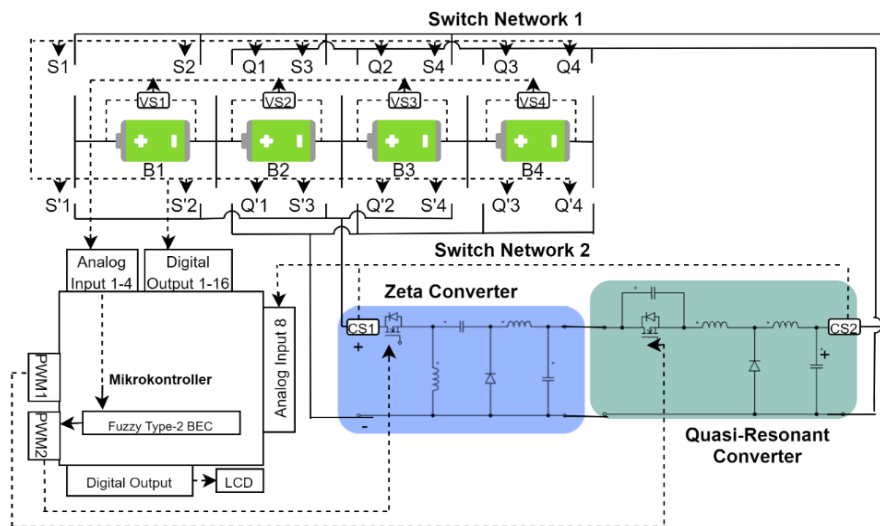


Figure 1. Diagram block of cell balancing system

Figure 2 shows the flowchart for the balancing system that will be carried out in this research. For the initial process, voltage sensors are read on each battery cell. Then the average voltage of each cell in the battery pack will be carried out. After averaging, if each battery 1, 2, 3, and 4 is less than the average voltage it will be used as a load. When each battery 1, 2, 3, and 4 has more than the average voltage it will be used as a source.

Table 1 gives the different possibilities of the switching topology. S'1 to S'4 and Q'1 to Q'4 are used as switches to connect the balancing circuit to the battery used as the source. S1 to S4 and Q1 to Q4 are used as switches to connect the balancing circuit to the battery used as a load. Next, after it is known which battery will be the source and load. Voltage reference is set in 4.2 which is max battery charging voltage. Then V_o will be obtained, and the V_o value will be compared with the reference voltage. If the V_o value and reference voltage are not the same, fuzzy type-2 control will be carried out to obtain the appropriate duty cycle. Then it is processed by getting the V_o value and comparing the V_o value with the reference voltage. When the V_o condition is the same as the reference voltage, the zeta converter output will produce the average voltage followed by a quasi-resonant converter which is used to smooth the zeta converter output ripple. Table 1 shows the sequence of switches used.

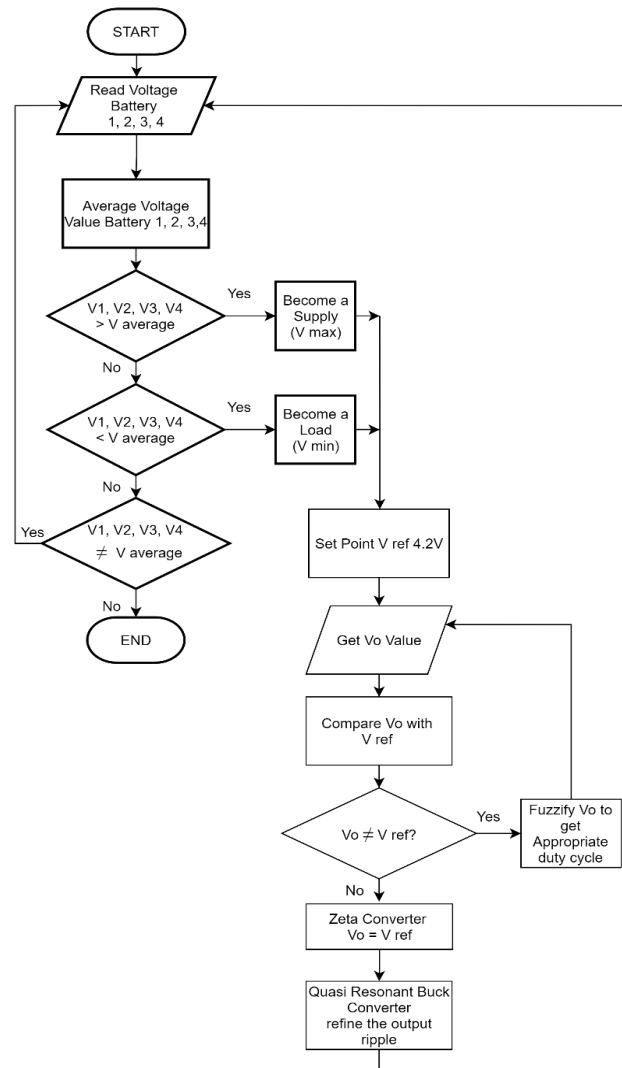


Figure 2. Flowchart system of cell balancing

Table 1. Sequential switch from relay of the cell balancing

Supply				Load				Input switch (Zeta)								Output switch (Quasi)							
B	B	B	B	B	B	B	B	S'	S'	S'	S'	Q'	Q'	Q'	Q'	S	S	S	S	Q	Q	Q	Q
1	2	3	4	1	2	3	4	1	2	3	4	1	2	3	4	1	2	3	4	1	2	3	4
1	0	0	0	0	1	0	0	1	0	0	0	1	0	0	0	0	1	0	0	0	1	0	0
0	1	0	0	1	0	0	0	0	1	0	0	0	0	1	0	0	1	0	0	1	0	0	0
0	0	1	0	1	0	0	0	0	0	1	0	0	0	0	1	0	0	0	0	1	0	0	0
0	0	0	1	1	0	0	0	0	0	0	1	0	0	0	1	1	0	0	0	1	0	0	0
1	0	0	0	0	0	1	0	1	0	0	0	1	0	0	0	0	0	1	0	0	0	1	0
0	1	0	0	0	0	1	0	0	0	1	0	0	0	1	0	0	0	1	0	0	0	1	0
0	0	1	0	0	1	0	0	0	0	1	0	0	0	1	0	0	1	0	0	0	1	0	0
0	0	0	1	0	1	0	0	0	0	0	1	0	0	0	1	0	1	0	0	0	1	0	0
1	0	0	0	0	0	0	1	1	0	0	0	1	0	0	0	0	0	0	1	0	0	0	1
0	1	0	0	0	0	0	1	0	1	0	0	0	1	0	0	0	0	0	1	0	0	0	1
0	0	1	0	0	0	0	1	0	0	1	0	0	0	1	0	0	0	0	1	0	0	0	1
0	0	0	1	0	0	1	0	0	0	0	1	0	0	0	1	0	0	1	0	0	0	1	0

2.1. Zeta converter modelling

Zeta converter represents a progression built upon the fundamental DC-DC converters circuit, enabling the conversion of a DC input into a variable DC output regulated by the duty cycle of the control circuit. It is structured by combining features of both the buck converter and boost converter, enabling it to raise or lower the output voltage. Zeta converter includes two inductors and a series capacitor in its circuit. Moreover, it utilizes an input capacitor to filter the input voltage and an output capacitor for filtering the output voltage.

Figure 3 depicts the circuit diagram of the zeta converter. The basic operation of the zeta converter is as follows: In mode 1, when MOS1 is in the on state, capacitor C_c is connected in series with L_2 . Energy from the input supply is stored in L_1 , L_2 , and C_c , with L_2 providing I_o . Figure 4(a) depicts the scenario during MOS1 being in the on state. In mode 2, with MOS1 in the Off state, the voltage across L_2 must be V_o , being parallel to C_{out} . As C_{out} is charged to V_o , the voltage across MOS1 aligns with V_o . Consequently, the voltage across L_1 is V_o about the drain of MOS1. Figure 4(b) illustrates this state when MOS1 is off [19].

The parameter of zeta converter is shown at Table 2. From Table 2, a zeta converter was obtained using the following equation.

$$D = \frac{V_{out}}{V_{out} + V_{in}} = 0.25$$

$$L_1 = \frac{1}{2} \times \frac{V_{in} \times D}{\Delta I_{L1} \times F} = 131.25 \mu H$$

$$L_2 = \frac{1}{2} \times \frac{V_{in} \times D}{\Delta I_{L2} \times F} = 70.31 \mu H$$

$$C_{out} = \frac{\Delta I_{L2}}{8 \times \Delta V_o \times F} = 70 \mu F$$

$$C_{in} = \frac{D \times I_{out}}{\Delta V_{cin} \times F} = 138 \mu F$$

$$C_c = \frac{D \times I_o}{\Delta V_{cc} \times F} = 416 \mu F$$

When V_{out} = output voltage (Volt), V_{in} = input voltage (volt), D = duty cycle (%), L = inductor (H), C_{out} = capacitor output (F), C_{in} = capacitor input (F), and C_c = capacitor coupling (F).

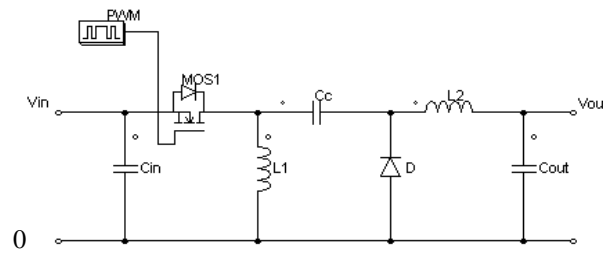


Figure 3. Circuit diagram of zeta converter

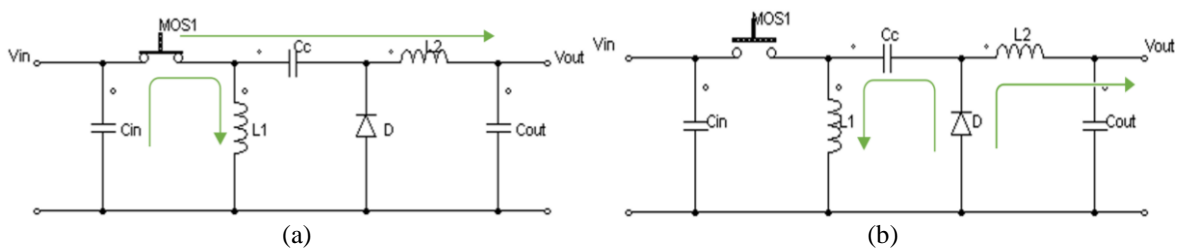


Figure 4. Basic operation of zeta converter in (a) mode 1 and (b) mode 2

Table 2. Zeta converter parameter

Parameter	Nominal	Unit	Parameter	Nominal	Unit
Input voltage (V_{in})	12.6	Volt	Inductor (L_1)	131.25	Henry
Input current (I_{in})	1.5	Ampere	Inductor (L_2)	70.31u	Henry
Output voltage (V_{out})	4.2	Volt	Input capacitor (C_{in})	138u	Farad
Output current (I_{out})	2.8	Ampere	Coupling capacitor (C_c)	416u	Farad
Switching frequency (F)	40k	Hertz	Output capacitor (C_{out})	70u	Farad

2.2. Quasi-resonant buck converter modeling

The quasi-resonant buck converter achieves a notable combination of high-power density and efficiency by facilitating commutation under zero voltage. The storage and transfer of energy from input to

output are accomplished through the utilization of an LC circuit. As a result, the regulation of quasi-resonant buck converters is achieved through frequency modulation (FM) [20].

Figure 5 illustrates the circuit diagram of the quasi-resonant buck converter, and its basic operation is detailed as in mode 1, represented in Figure 6(a), the process begins with a loss of pulse on the gate of MOS, initiating the flow of current through Cr. The voltage on MOS1 progressively increases. Moving to mode 2, as depicted in Figure 6(b), D1 is turned on, generating I_o through the quasi-inductor and buck-inductor currents. This mode involves resonance in the resonant circuit, causing the capacitor voltage to surpass the input voltage, reducing the current flow through the inductor. Once the capacitor reaches its peak voltage and the inductor current becomes zero, the capacitor releases power, forcing the inductor current in a different direction. In mode 3, presented in Figure 6(c), after the capacitor is fully charged, there may still be residual energy in the inductor. The diode on the MOS1 body activates, allowing the remaining energy to flow through this diode. The final mode 4, shown in Figure 6(d), involves supplying voltage to the gate of MOS1, turning off D1. This results in an increased current flow through MOS1, concluding when the gate of MOS1 loses its pulse for the next cycle [21].

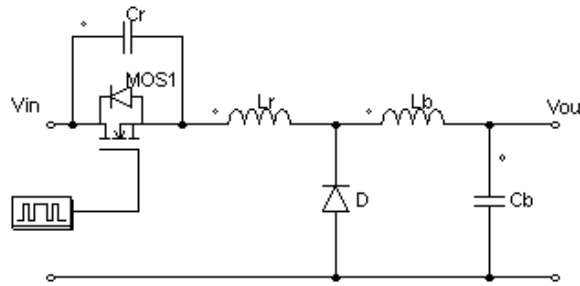


Figure 5. Circuit diagram of quasi-resonant buck converter

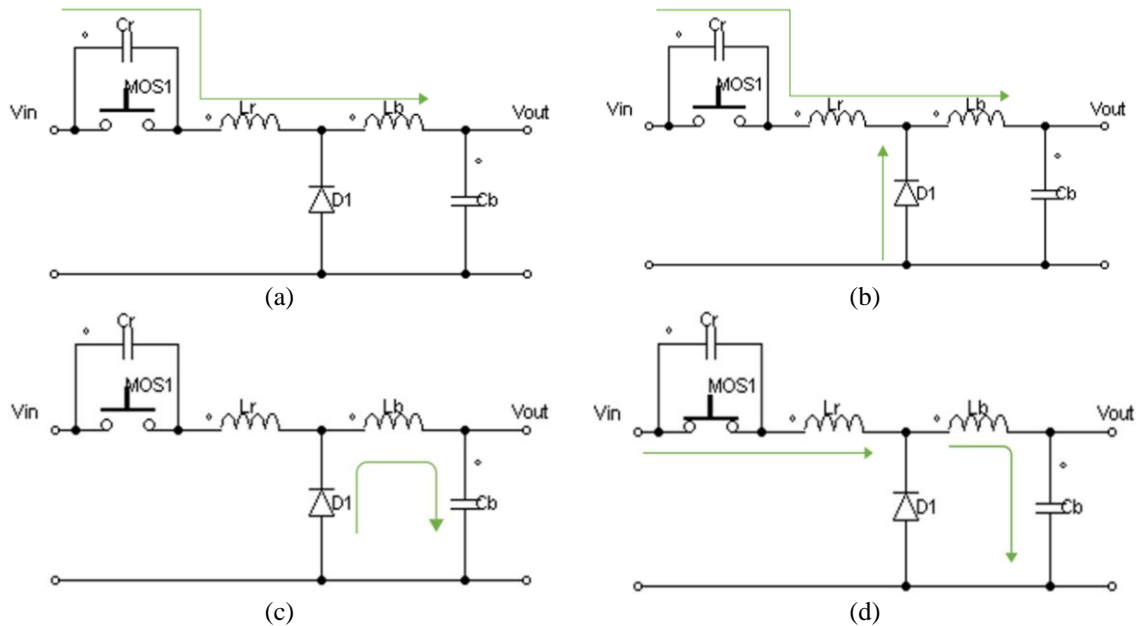


Figure 6. Basic operation of quasi-resonant buck converter in (a) mode 1, (b) mode 2, (c) mode 3, and (d) mode 4

The parameter of the quasi-resonant buck converter is shown in Table 3. From Table 3 Quasi-resonant buck converter was obtained using the following equation:

$$C_r = \frac{1}{2\pi FZ} = 1.11\mu F$$

$$L_r = \frac{Z}{2\pi F} = 14\mu H$$

$$D = \frac{V_{out}}{V_{in}} = 0.42$$

$$L_b = \frac{(1-D) V_{out}}{\Delta I_{L2} \times F} = 147.41 \mu H$$

$$C_b = \frac{(1-D)}{8Lb \left(\Delta V_{out} / V_{out} \right) F^2} = 82 \mu F$$

When V_{out} = output voltage (volt), V_{in} = input voltage (volt), D = duty cycle (%), L_r = inductor quasi-resonant (H), C_r = capacitor output (F), L_b = inductor buck (H), and C_b = capacitor buck (F).

Table 3. Quasi-resonant buck converter parameter

Parameter	Nominal	Unit	Parameter	Nominal	Unit
Input voltage	4.2	Volt	Inductor L_r	1.11	Henry
Output voltage	4.2	Volt	Inductor L_b	1472.81u	Henry
Output current	2.8	Ampere	Capacitor C_r	14u	Farad
Switching frequency	40 k	Hertz	Capacitor C_b	100u	Farad
Resonant frequency	40 k	Hertz			

2.3. Fuzzy type-2-BEC

Fuzzy logic controller (FLC) is already used in various engineering applications. The FLCs changed from conventional methods to a decision-making system with strong reasoning in a limited number of rules [18]. Fuzzy type-1 is a type that is widely used nowadays. However, fuzzy type-1 can only handle a limited level of uncertainty, whereas applications are often faced with many sources with a high level of uncertainty. Fuzzy type-2 was created to improve the fuzzy type-1 system. Fuzzy type-2 is considered potentially better for modeling uncertainty [22]. In fuzzy type-2 there are four main processes shown in Figure 7.

In the provided Figure 7, several stages are outlined for determining the fuzzy type-2 output. The initial phase in the design of fuzzy type-2 involves establishing input parameters during identification. The resulting fuzzy output is a duty cycle designed to align the voltage output from the zeta converter with a specified set point: set point = 4.2 V, error = -4.2 V to 4.2 V, and delta error = -8.4 V to 8.4 V.

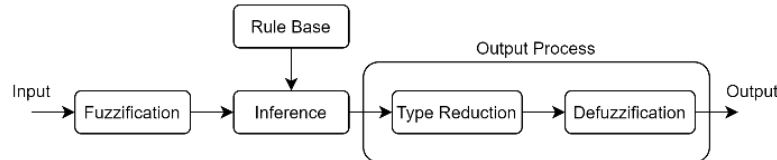


Figure 7. Fuzzy type-2 block diagram system

Fuzzification is a process implemented to transform variables into fuzzy variables. The predetermined input data, presented in a crisp form as errors and delta errors, undergoes conversion to fuzzy sets for utilization in calculating the truth value of the premise within each rule. The decision-making process involves selecting fuzzy sets to determine both input and output by converting crisp sets into fuzzy language. As depicted in Figures 8(a) and 8(b), fuzzy control employs two inputs: "error" (set point until the present value) and "delta error" (current error until previous error). The fundamental rule governing fuzzy logic decision-making relies on an IF-THEN rule-based system, where IF represents the cause and THEN signifies the effect. IF-THEN statements are commonly employed in fuzzy rules (rule base) to articulate actions in response to diverse fuzzy inputs. These rules are represented in the linguistic table format of membership functions, aligning with the overall behavior of the system. The rules can be structured as a matrix, exemplified in Figures 8(a) and (b), where 49 rules determine the output value for the single-tone response, based on the seven membership functions of input error and delta error [23]. The process of mapping firm values from input into a fuzzy set using membership functions. Input values are mapped into membership degrees using the following function:

$$(x; a, b, c) \left\{ \begin{array}{ll} 0, & x \leq a \\ \frac{x-a}{b-a}, & a < x \leq b \\ \frac{c-x}{c-b}, & b < x \leq c \\ 0, & c < x \end{array} \right\}$$

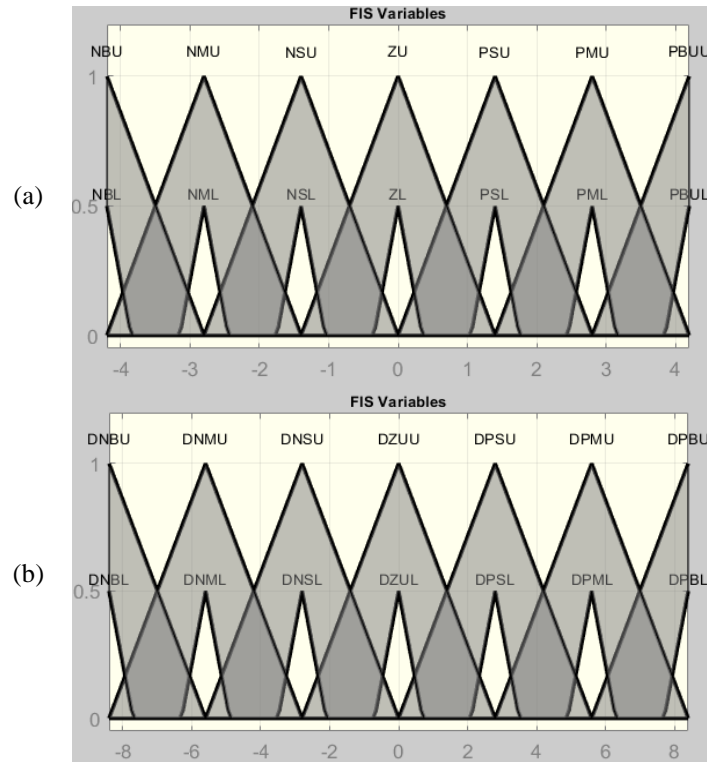


Figure 8. Design of membership function input: (a) error and (b) delta error

Fuzzy inference involves establishing the mapping from input to output in fuzzy logic. The output duty cycle's membership function in this study encompasses seven types of single tones: negative big (NB), negative medium (NM), negative small (NS), zero (Z), positive small (PS), positive medium (PM), and positive big (PB). The defuzzification process aims to convert the fuzzy variable back into a conventional real variable, essentially transforming the initially represented fuzzy control action into a singular numerical value. The output of each rule is directly correlated with the input variable linearly. This defuzzification procedure is designed to determine the precise numerical outcome of the computation, often referred to as the "crunch value" [24]. Table 4 guides the selection of a 7×7 rule base in a fuzzy system, taking into account the complexity of the problem and the necessary input combinations to achieve desired outcomes. While a larger rule base offers greater flexibility in depicting the relationship between input and output variables, it also introduces heightened complexity and computational demands [25].

Table 4. Fuzzy type-2 rule base

dE/E	NB	NM	NS	Z	PS	PM	PB
NB	NB	NB	NB	NB	NM	NS	Z
NM	NB	NB	NM	NM	NS	Z	PS
NS	NB	NM	NS	NS	Z	PS	PM
Z	NB	NM	NS	Z	PS	PM	PB
PS	NM	NS	Z	PS	PS	PM	PB
PM	NS	Z	PS	PM	PM	PB	PB
PB	Z	PS	PS	PB	PB	PB	PB

3. RESULTS AND DISCUSSION

In this section, there will be the result of the simulation experiment using MATLAB R2022b. Fuzzy type-2 is used to obtain duty cycle values to ensure the voltage of the converter is stable according to the set point 16 relays were installed in this circuit 8 connected with the zeta converter's input and 8 others connected to the quasi-resonant output. The system used to regulate relay ignition is the min and max values. The cut-off value will cut off when the battery voltage is the same as the average of the four batteries. Figure 9 shows the overall system consisting of the main circuit and control circuit.

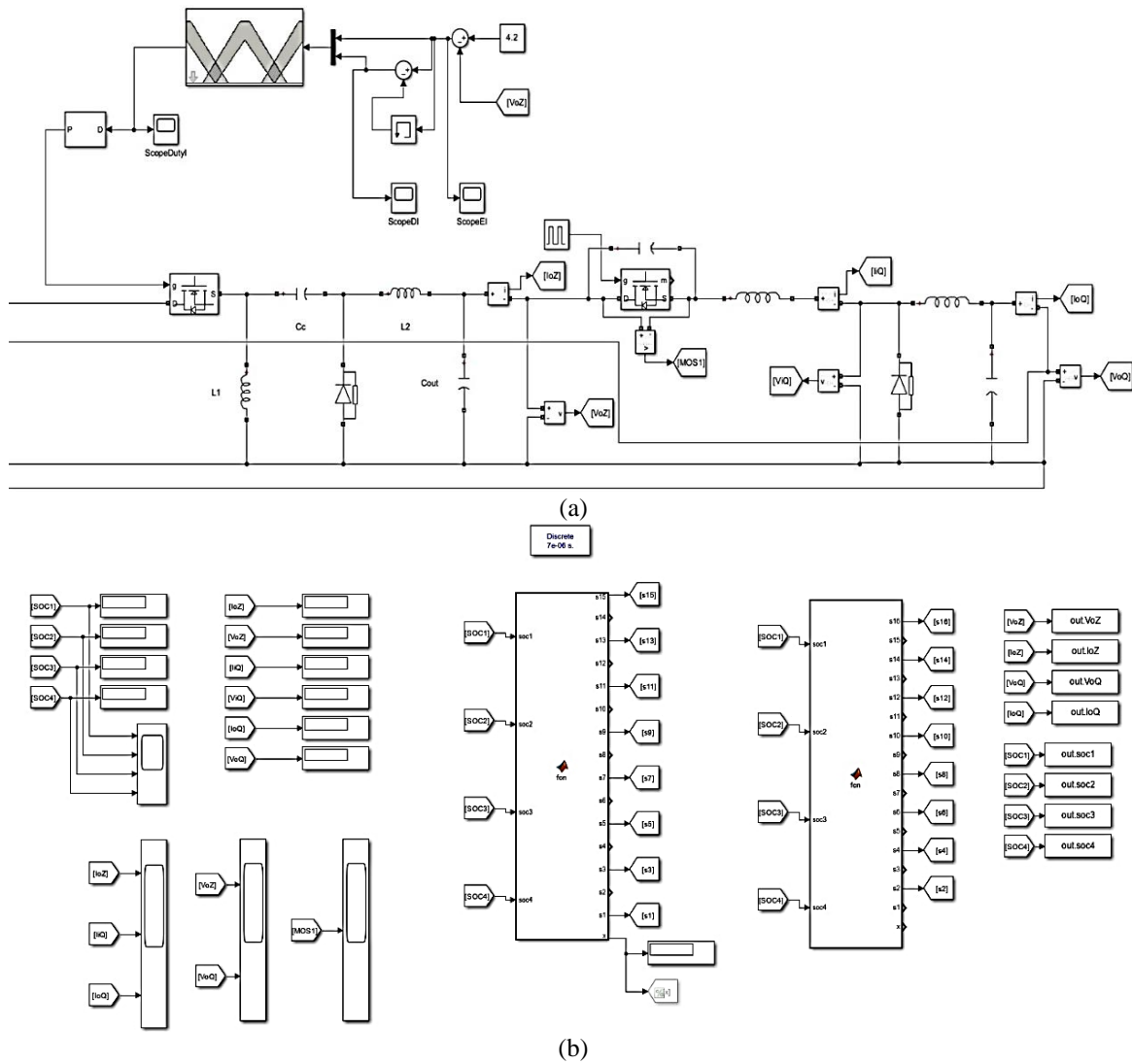


Figure 9. Overall system: (a) main circuit and (b) control circuit

There will be 2 variations to balance the battery cell. In the first variation, battery 1 is set at SOC 50%, battery 2 is set at SOC 53%, battery 3 is set at SOC 52%, and battery 4 is set at SOC 54%. Fuzzy type-2 is set at the battery voltage average. All battery cells are balanced at 60 s, as seen in Figure 10, and balanced at the battery SOC average which is 52.2591%.

In Figure 11, the V_o quasi-resonant buck converter is stable at 3.97 V. There's an oscillation at 46 s and 54 s, it happens because there's a change in the load and sources, and the control can bring out the oscillation to stable at 3.97 V. Table 5 shows the data from time 0 s to 60 s until all cell batteries are balanced. In the process of balancing, there's a difference between the start cell average and the end cell average. This difference is due to losses that occur during the balancing process. In the balancing process carried out, there is a percent error of the SOC average from the start process to the end are 0.45%.

In the second variation, battery 1 is set at SOC 60%, battery 2 is set at SOC 57%, battery 3 is set at SOC 55%, and battery 4 is set at SOC 53%. All battery cells are balanced at 150s, as seen in Figure 12, and balanced at the battery SOC average which is 55.6415%. In Figure 13, the V_o quasi resonant buck converter is stable at 3.97 V. There's an oscillation at 110 s and 122 s, it happens because there's a change in the load and sources, and the control can bring out the oscillation to stable at 3.97 V. Table 6 shows the data from time 0s to 150 s until all cell batteries are balanced. In the process of balancing, there's a difference between the start cell average and the end cell average. This difference is due to losses that occur during the balancing process. In the balancing process carried out, there is a percent error of the SOC Average from the start process to the end are 1.082%.

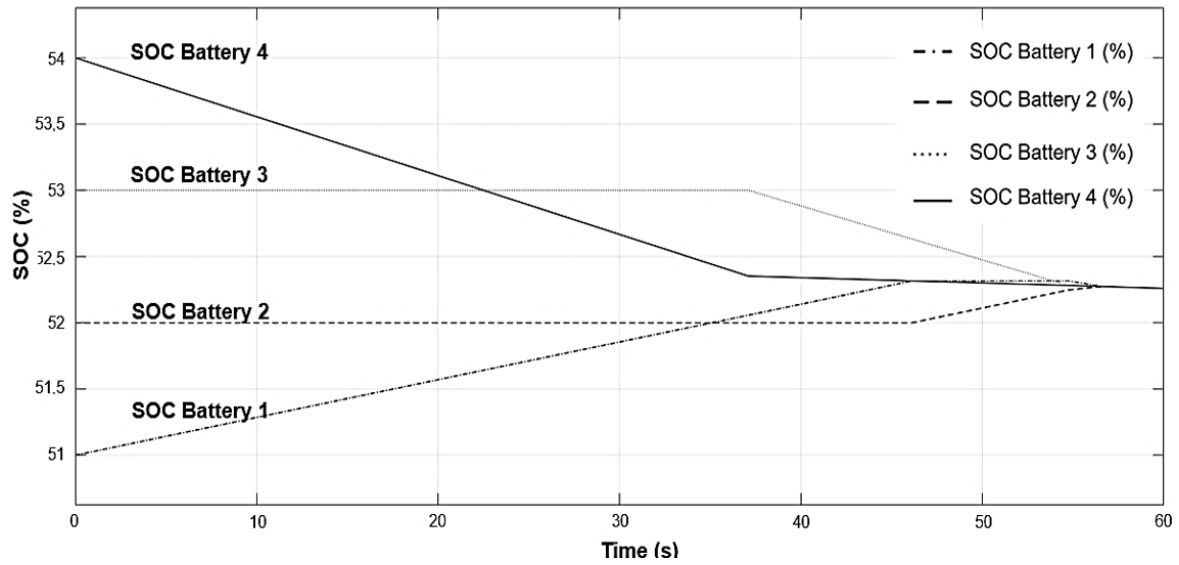


Figure 10. Graphic cell balancing variation one

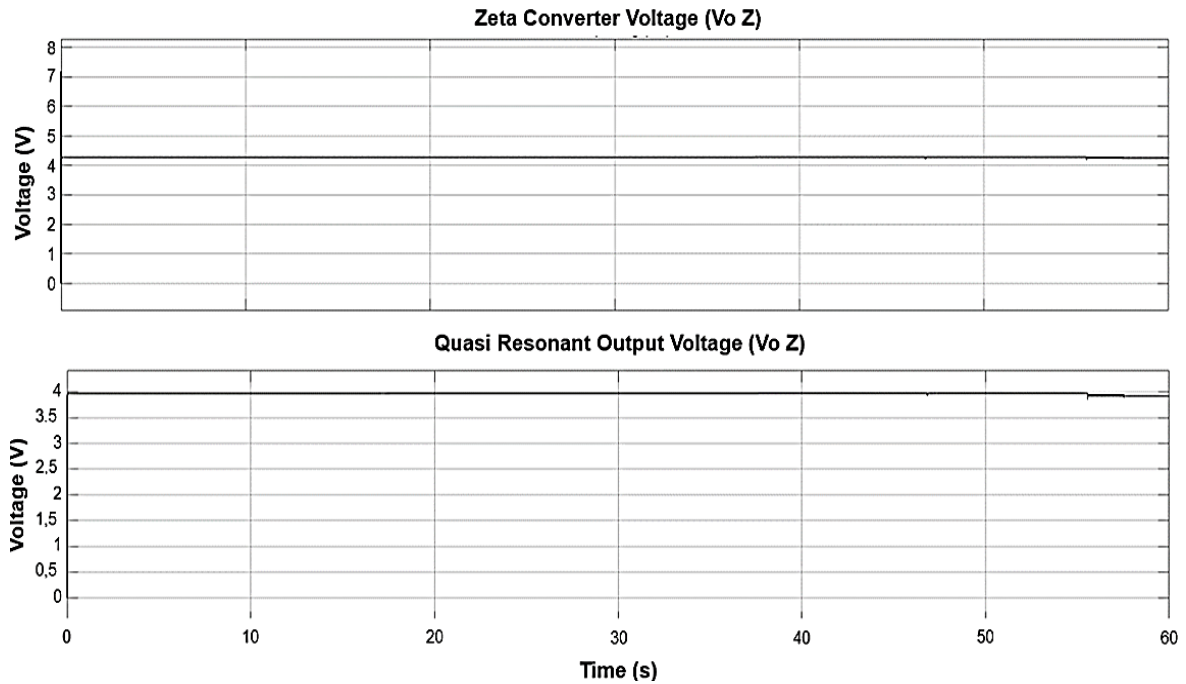


Figure 11. Graphic zeta output voltage and quasi output voltage in variation one

Table 5. Cell balancing variation one result

Time (s)	Vo Quasi (V)	Io Quasi (A)	Batt 1 SOC (%)	Batt 2 SOC (%)	Batt 3 SOC (%)	Batt 4 SOC (%)	SOC Average (%)
0	8.13E-06	9.69E-05	51	53	52	54	52.5
10	3.9705	3.0805	51.285	53	52	53.555	52.46
20	3.9709	3.077	51.570	53	52	53.111	52.42
30	3.9713	3.0734	51.854	53	52	52.667	52.38
40	3.9726	3.1017	52.140	52.881	52	52.340	52.34
50	3.9724	3.0977	52.316	52.474	52.111	52.300	52.3
60	3.9187	3.3414	52.259	52.259	52.259	52.259	52.259

Table 6. Cell balancing variation two result

Time (s)	Vo Quasi (V)	Io Quasi (A)	Batt 1 SOC (%)	Batt 2 SOC (%)	Batt 3 SOC (%)	Batt 4 SOC (%)	SOC Average (%)
0	8.13E-06	9.7E-05	60	57	55	53	56.25
10	3.9748	3.1048	59.552	57	55	53.287	56.2
20	3.9752	3.1018	59.104	57	55	53.574	56.16
30	3.9756	3.0986	58.656	57	55	53.861	56.12
40	3.9760	3.0953	58.209	57	55	54.148	56.08
50	3.9764	3.0922	57.763	57	55	54.435	56.04
60	3.9769	3.0893	57.316	57	55	54.721	56
70	3.9773	3.0867	57.871	57	55	55.007	56.36
80	3.9777	3.0838	56.425	57	55	55.292	55.92
90	3.9780	3.0806	55.980	57	55	55.578	55.88
100	3.9781	3.1092	55.849	56.683	55.013	55.851	55.849
110	3.9784	3.1064	55.809	56.275	55.301	55.851	55.809
120	3.9788	3.1039	55.769	55.867	55.589	55.851	55.769
130	3.97224	3.3441	55.727	55.727	55.727	55.851	55.758
140	3.9221	3.3453	55.684	55.684	55.684	55.684	55.684
150	3.9222	3.3437	55.641	55.641	55.641	55.641	55.641

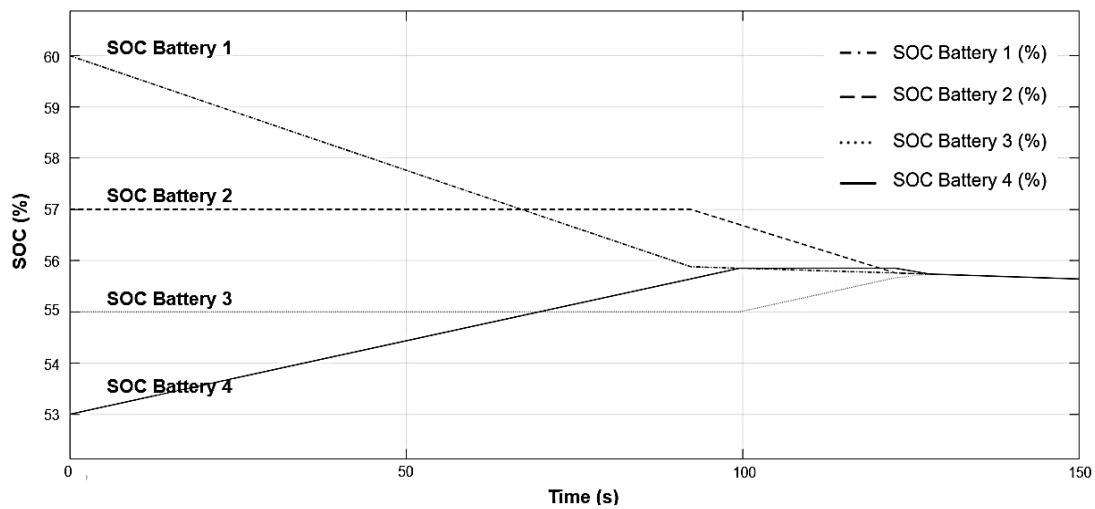


Figure 12. Graphic cell balancing variation two

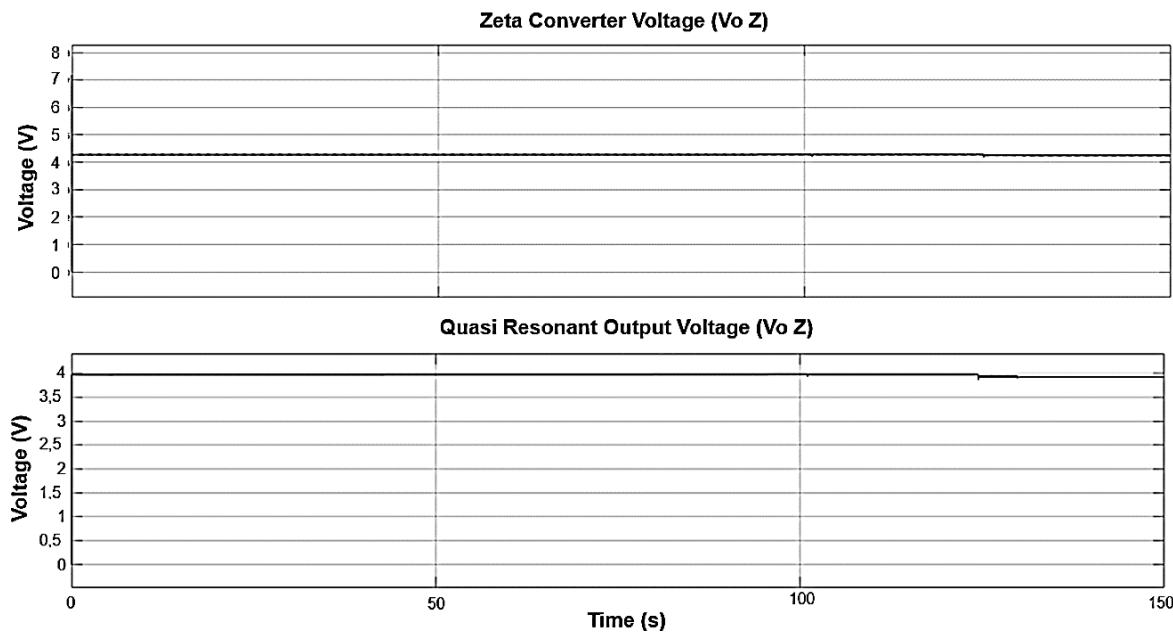


Figure 13. Graphic zeta output voltage and quasi output voltage in variation two




4. CONCLUSION

After doing the balancing test with two variations, the cell-to-cell active balancing using fuzzy type-2 battery equalizer controller (BEC) implemented zeta converter and quasi-resonant buck converter on battery pack Li-ion succeeded in balancing all cells with constant voltage at 3.97 V. There's an oscillation at the Voltage output of both converters, it happens because there's a change in the load and sources, and the control can bring out the oscillation to stable at 3.97 V. There's an error in the average of the balancing process. This difference is due to losses that occur during the balancing process. In the balancing process carried out, there is a percent error of the SOC Average from the start process to the end in variation one 0.45% and variation two 1.082%.




REFERENCES

- [1] W. Zhang, X. Fang, and C. Sun, "The alternative path for fossil oil: Electric vehicles or hydrogen fuel cell vehicles?," *Journal of Environmental Management*, vol. 341, 2023, doi: 10.1016/j.jenvman.2023.118019.
- [2] X. Sun, Z. Li, X. Wang, and C. Li, "Technology Development of Electric Vehicles: A Review," *Energies*, vol. 13, no. 1, p. 90, Dec. 2019, doi: 10.3390/en13010090.
- [3] J. Duan *et al.*, "Building Safe Lithium-Ion Batteries for Electric Vehicles: A Review," *Electrochemical Energy Reviews*, vol. 3, no. 1, pp. 1–42, Mar. 2020, doi: 10.1007/s41918-019-00060-4.
- [4] J. Wen, D. Zhao, and C. Zhang, "An overview of electricity powered vehicles: Lithium-ion battery energy storage density and energy conversion efficiency," *Renewable Energy*, vol. 162, pp. 1629–1648, 2020, doi: 10.1016/j.renene.2020.09.055.
- [5] T. Horiba, "Lithium-Ion Battery Systems," in *Proceedings of the IEEE*, Jun. 2014, vol. 102, no. 6, pp. 939–950, doi: 10.1109/JPROC.2014.2319832.
- [6] A. G. Olabi, Q. Abbas, P. A. Shinde, and M. A. Abdelkareem, "Rechargeable batteries: Technological advancement, challenges, current and emerging applications," *Energy*, vol. 266, 2023, doi: 10.1016/j.energy.2022.126408.
- [7] V. Dimitrov and N. Pavlov, "Study of the Starting Acceleration and Regenerative Braking Deceleration of an Electric Vehicle at Different Driving Modes," 2021, doi: 10.1109/BulEF53491.2021.9690780.
- [8] Z. B. Omariba, L. Zhang, and D. Sun, "Review of Battery Cell Balancing Methodologies for Optimizing Battery Pack Performance in Electric Vehicles," *IEEE Access*, vol. 7, pp. 129335–129352, 2019, doi: 10.1109/ACCESS.2019.2940090.
- [9] K. Khaeruddin, W. Wijono, and R. N. Hasanah, "Desain Penyeimbangan Sel Baterai Lithium-Ion dengan Teknik Cell-to-Cell Charging Mode pada Battery Management System (BMS)," *Jurnal Ecotipe (Electronic, Control, Telecommunication, Information, and Power Engineering)*, vol. 8, no. 1, pp. 9–15, 2021, doi: 10.33019/jumalecotipe.v8i1.2137.
- [10] R. Paidi and S. K. Gudey, "Active and Passive Cell Balancing Techniques for Li-Ion Batteries used in EVs," 2022, doi: 10.1109/IPRECON55716.2022.10059573.
- [11] S. Hemavathi, "Overview of cell balancing methods for Li-ion battery technology," *Energy Storage*, vol. 3, no. 2, Apr. 2021, doi: 10.1002/est2.203.
- [12] D. Thiruvonasundari and K. Deepa, "Optimized Passive Cell Balancing for Fast Charging in Electric Vehicle," *IETE Journal of Research*, vol. 69, no. 4, pp. 2089–2097, May 2023, doi: 10.1080/03772063.2021.1886604.
- [13] S. Kumar, S. K. Rao, A. R. Singh, and R. Naidoo, "Switched-Resistor Passive Balancing of Li-Ion Battery Pack and Estimation of Power Limits for Battery Management System," *International Journal of Energy Research*, vol. 2023, 2023, doi: 10.1155/2023/5547603.
- [14] S. Singirikonda and Y. P. Obulesu, "Active cell voltage balancing of Electric vehicle batteries by using an optimized switched capacitor strategy," *Journal of Energy Storage*, vol. 38, p. 102521, Jun. 2021, doi: 10.1016/j.est.2021.102521.
- [15] Y. Shang, C. Zhang, N. Cui, and J. M. Guerrero, "A cell-to-cell battery equalizer with zero-current switching and zero-voltage gap based on quasi-resonant lc converter and boost converter," *IEEE Transactions on Power Electronics*, vol. 30, no. 7, pp. 3731–3747, 2015, doi: 10.1109/TPEL.2014.2345672.
- [16] S. L. Wu, H. C. Chen, and C. H. Chien, "A novel active cell balancing circuit and charging strategy in lithium battery pack," *Energies*, vol. 12, no. 23, 2019, doi: 10.3390/en12234473.
- [17] B. Jiang, "Active Cell Balancing Algorithms in Lithium-ion Battery," 2020.
- [18] A. Sarkar, R. Dutt, S. Sahu, and A. Acharyya, "Energy-efficient and High Speed Active Cell Balancing Methodology for Lithium-ion Battery Pack," 2023, doi: 10.1109/NEWCAS57931.2023.10198124.
- [19] J. Falin, "Designing DC/DC Converters based on ZETA Topology," *Analog Applications Journal Texas Instruments Incorporated*, vol. 2Q, pp. 16–21, 2010.
- [20] N. Hinov, "Model-Based Design of a Buck ZVS Quasi-Resonant DC-DC Converter," 2022, doi: 10.1109/HiTech56937.2022.10145536.
- [21] V. Wuti, A. Luangpol, K. Tattiwong, S. Trakuldit, A. Taylim, and C. Bunlaksananusorn, "Analysis and design of a zero-voltage-switched (ZVS) quasi-resonant buck converter operating in full-wave mode," 2020, doi: 10.1109/ICEAST50382.2020.9165351.
- [22] C. Dumitrescu, P. Ciotirnae, and C. Vizitiu, "Fuzzy logic for intelligent control system using soft computing applications," *Sensors*, vol. 21, no. 8, 2021, doi: 10.3390/s21082617.
- [23] Y. Shekhar and A. U. Ahmad, "A Performance Comparison Study of Hybrid Electric Vehicle between Type-1 and Interval Type-2.0 FLC," 2023, doi: 10.1109/PIECON56912.2023.10085834.
- [24] A. Meylani and A. S. Handayani, "Perbandingan Kinerja Sistem Logika Fuzzy Tipe-1 dan Interval Tipe-2 pada Aplikasi Mobile Robot," *Computer Science and ICT*, vol. 3, no. 1, pp. 209–214, 2017.
- [25] K. Mittal, A. Jain, K. S. Vaisla, O. Castillo, and J. Kacprzyk, "A comprehensive review on type 2 fuzzy logic applications: Past, present and future," *Engineering Applications of Artificial Intelligence*, vol. 95, 2020, doi: 10.1016/j.engappai.2020.103916.




BIOGRAPHIES OF AUTHOR

Indhana Sudiharto    was born in Madiun, Indonesia in 1966. He received a bachelor of engineering degree in power system from Sepuluh Nopember of Institute of Technology, Indonesia in 1996, and a master of engineering degree in Power System from Sepuluh Nopember of Institute of Technology, Indonesia in 2006. He is currently an associate professor with the Department of Electrical Engineering, Politeknik Elektronika Negeri Surabaya (PENS), Indonesia. He joined the Division of Industrial Electrical Engineering, Department of Electrical Engineering, Politeknik Elektronika Negeri Surabaya (PENS), Indonesia, as a lecturer, in 1996. He heads the research group of power quality PENS. His research interests include power systems, renewable energy, and power electronics. As a lecturer, he has taught subjects such as electrical measurement and instrumentation, electrical power system protection, and power quality. He can be connected at email: indhana@pens.ac.id.



Farid Dwi Murdianto    was born in Malang, Indonesia in 1991. He received the bachelor degree in Applied Engineering in Industrial Electrical from Politeknik Elektronika Negeri Surabaya (PENS), Indonesia in 2013 and the master of engineering degree in Power System from Sepuluh Nopember of Institute of Technology, Indonesia in 2015. He is currently a Head of Central Intellectual Property Rights at Politeknik Elektronika Negeri Surabaya (PENS), Indonesia. He joined the Division of Industrial Electrical Engineering, Department of Electrical Engineering, Politeknik Elektronika Negeri Surabaya (PENS), Indonesia, as a lecturer, in 2015. He joined several research groups including Power Quality, Energy Conservation and Power Electronic, and Electric Drive at PENS. His research interests include renewable energy and power electronics. As a lecturer, he has taught subjects such as renewable energy, power quality and microcontrollers. He can be connected at email: farid@pens.ac.id.



Vena Chika Widyasavitta    was born in Sidoarjo, Indonesia in 2001. She currently pursuing a bachelor's degree in Applied Engineering at Industrial Electrical from Politeknik Elektronika Negeri Surabaya (PENS), Indonesia in 2024. Currently, she is doing final project research in power electronics, specifically balancing systems. Her areas of interest include power electronics, renewable energy control systems, and power quality. She can be connected at email: venachika@gmail.com.